

Charge qubits and limitations of electrostatic quantum gates

A. Weichselbaum and S. E. Ulloa

Department of Physics and Astronomy, Nanoscale and Quantum Phenomena Institute, Ohio University, Athens, Ohio 45701-2979

(Date: 22 Dec 2003)

We investigate the characteristics of purely electrostatic interactions with external gates in constructing full single qubit manipulations. The quantum bit is naturally encoded in the spatial wave function of the electron system. Single-electron-transistor arrays based on quantum dots or insulating interfaces typically allow for electrostatic controls where the inter-island tunneling is considered constant, e.g. determined by the thickness of an insulating layer. A representative array of 3×3 quantum dots with two mobile electrons is analyzed using a Hubbard Hamiltonian and a capacitance matrix formalism. Our study shows that it is easy to realize the first quantum gate for single qubit operations, but that a second quantum gate only comes at the cost of compromising the low-energy two-level system needed to encode the qubit. We use perturbative arguments and the Feshbach formalism to show that the compromising of the two-level system is a rather general feature for electrostatically interacting qubits and is not just related to the specific details of the system chosen. We show further that full implementation requires tunable tunneling or external magnetic fields.

PACS numbers: 03.67.Lx, 02.70.-c, 85.35.Be, 85.35.Gv

I. INTRODUCTION

Quantum computation in its binary concept requires a set of two different quantum states, a *quantum two-level system* (qu2LS), that realizes the quantum bit physically [1]. Some physical systems are intrinsically qu2LSs such as the spin 1/2 of a fermion or the polarization of a photon. Spin 1/2 systems such as some nuclei of atoms or electrons are considered well-suited also because of the comparatively long spin decoherence times (\sim ms to ns) [2, 3, 4] which derives from the rather weak interaction of the spin with its environment. This long coherence also has the price that important processes in qubit operation are rather slow processes. On the other hand, decoherence times for charge based quantum systems are orders of magnitude shorter (\sim ns) due to the comparatively strong Coulomb interaction [5, 11]. Yet, all quantum gates including interacting qubits can be expected to scale similarly in time and to allow for fast qubit operations well below the decoherence limits. Furthermore, final readout through single-electron transistors (SET) or quantum point contacts (QPC) appears to be “straight-forward” (i.e., implementable in principle) [6, 7, 8].

In this paper we discuss quantum bits (qubits) encoded in the spatial wave function of electrons embedded in condensed matter systems, and the emphasis is placed on whether it is possible to realize a qubit based solely on charge distribution (*charge qubit*) and capacitive coupling. For example, having a set of two quantum dots (qudots) close enough so that one electron can tunnel back and forth, one may envisage a qubit where the electron being on one quantum dot (qudot) represents one state, and being on another qudot the other state [5]. Other examples are the cellular automata setups with a 2×2 array of qudots with excess electrons [9, 10]. These proposals are fundamentally based on the variability of the tunneling t . Yet there are many physical quantum

systems where the handle on the tunneling is limited or non-existent, such as the case of metallic qudot structures where the tunneling barrier is determined by the thickness of oxide layers in the structure.

This then suggests the question of whether there is a way that electrostatically controlled logical quantum gates (qugates) can realize the necessary single qubit operations and the tunability of interactions between them. In this context, it is important to clearly define what one means by a quantum bit encoded in a quantum two-level system (qu2LS) and what are the requirements for it. The following criteria are established for the usefulness of a qu2LS [1]:

- A1. The qu2LS should include the ground state of the system in the *working-range* of the (tunable) parameters; this clearly facilitates the initialization process in an experiment and is much more reliable when compared to a qu2LS completely built on excited states.
- A2. The qu2LS should be well separated in energy from the remaining states in the Hilbert space. This reduces the influence of the remaining Hilbert space, whose interference can be insofar interpreted as a source of *decoherence* and transitions to which may result in loss of probability in the primary system. This *lossy channel* for the qu2LS is considered in more detail below.
- A3. The qu2LS must interact with a set of external gates in order to control single qubit states as well as the interaction between them without compromising the two-level system.

In the case of charge located on a set of well-defined quantum dots (a *qudot network*), the electrostatic interaction is clearly able to satisfy point (A3) where Coulomb blockade (or charging) effects introduce a high energy

scale ($\gtrsim 1\text{meV}$) in typical qudots. These structures localize the operating electrons and limit the unwanted fast decoherence times due to interaction with the surrounding condensed matter environment. Typical decoherence sources such as phonons or unstable impurities in the environment are regarded frozen out or static, respectively, at the low temperatures required for operation of the qubit system. Consequently, the primary source of decoherence in this regime is in fact the reservoir of high-lying states, and its coherent interference with the qu2LS will be considered explicitly in our description.

The effect of the controlling electrostatic gates on the *reservoir* of high-lying states must be in the adiabatic regime. The time dependent manipulation through gate action can be estimated in the following manner: the gates are considered to act in clearly specified time windows in a step like behavior: they are turned on and off at will. This switching, however, is always carried out with a maximum speed which introduces a characteristic frequency $\omega_{switch} = 2\pi/\tau_{switch}$, where τ_{switch} is the switching time itself. In order for the influence of the reservoir of higher lying states to be negligible, $\hbar\omega_{switch}$ must be much smaller than the energy difference to the closest coupled states in that bath; thus the switching must be done smoothly enough (adiabatically), so as to not admix higher states into the lower qubit states. Coherent quantum operation in the qu2LS, however, demands the switching to be done faster than $1/\delta$, where δ is the splitting of the qu2LS in question, and incorporated in criterion (A2).

With respect to criteria (A2) and (A3), an estimate of how much of the wave function may be lost for each gate operation can be obtained from the Feshbach formalism [14]. For the unperturbed low-energy state manifold \mathcal{P} (in contrast to the remainder of the space \mathcal{Q}), an initial state $|\psi\rangle$ fully contained in \mathcal{P} will acquire projections in \mathcal{Q} due to a gate operation V (assumed instantaneous), given by

$$\langle\psi_{\mathcal{Q}}|\psi_{\mathcal{Q}}\rangle = \langle\psi_{\mathcal{P}}|H_{PQ}\frac{1}{E-H_{QQ}}\cdot\frac{1}{E-H_{PQ}}H_{QP}|\psi_{\mathcal{P}}\rangle,$$

where $H = H_0 + V$ and $H_{PQ} \equiv PHQ$ is a projection of the Hamiltonian, and with the other projections defined similarly (see Eq. (4) below). Space \mathcal{Q} is considered to be at least an energy Δ_0 separated from space \mathcal{P} and the change in the matrix elements due to the gate operation V is approximated by the splitting δ induced by that very V in the ground state pair in \mathcal{P} ; with this, the equation above can be estimated as

$$\langle\psi_{\mathcal{Q}}|\psi_{\mathcal{Q}}\rangle \lesssim \langle\psi_{\mathcal{P}}|\left(\frac{\delta}{\Delta_0}\right)^2|\psi_{\mathcal{P}}\rangle = \left(\frac{\delta}{\Delta_0}\right)^2. \quad (1)$$

The gate operations considered are a sequence of steps in the external parameters, which implies that with every one of these steps a small probability fraction is lost from the ground qu2LS to the remaining higher lying states, and as such it can be considered as an additional

channel for decoherence, even if the projection is nearly reversible in a gate cycle. Moreover, if the ground state can be considered sufficiently isolated ($\delta \ll \Delta$), the error drops quadratically with the ratio δ/Δ , so that if $\delta \simeq 0.03\Delta$, the probability lost per gate operation would be smaller than 0.1 %. However, because the gate operations will never be performed instantaneously – smoothing the transitions so that they take longer than Δ_0^{-1} but are faster than δ^{-1} – this is clearly to reduce the probability loss to the ‘ \mathcal{Q} reservoir’ of excited states.

Thus with proper adiabatic design of the qugates with respect to the higher lying ‘reservoir’, the way to single qubit operations is open. However, how exactly these are realized still leaves plenty of possibilities, which one can imagine being flexible enough. Here the main emphasis is placed on capacitively coupled quantum gates and the question of whether they allow the necessary single qubit operations. Most surprisingly, the answer will turn out negative. Despite the great degree of flexibility in geometry of electrostatic gates and system design, we will show below that it is not possible to implement fully operational qugates without compromising the robustness of the qubits.

II. THE MODEL SYSTEM

The model network under consideration is a 3×3 array of qudots with a single state per site and spin included. For theoretical purposes the structure is taken large enough to illustrate the main physics. For an experiment in this area, however, it is likely more practical to choose an array with fewer dots and gates. For the analysis, the 3×3 array is flexible and manageable, and is used to illustrate our generalized conclusions. Other geometries have been explored and yield similar results.

The 3×3 array of qudots is sketched together with the set of external gates in Fig. 1a. As seen from panel (b), only nearest neighbor capacitances are taken into account as well as nearest neighbor tunneling between dots. Overall, four parameters enter the model: the capacitance from each dot to either one of the gates ($C_g = 45\text{aF}$), the nearest-neighbor dot-dot capacitance ($C_{dd} = 45\text{aF}$), the dot self capacitance ($C_{d0} = 45\text{aF}$) and the nearest neighbor dot-dot tunneling ($t \sim 2\mu\text{eV}$). For these values, the energy cost for double occupancy (the Hubbard U) becomes $U = 1\text{meV}$, a typically used value in this context. Including a dielectric constant of $\epsilon = 10$, these numbers represent a typical design where dots of size 200nm are separated by approximately also 200nm. These numbers can of course change depending on the detailed geometry and shapes of the dots. In that sense, the circles in Fig. 1a are just a symbolic representation of the dots. However, the capacitance values chosen correspond to relatively large nano-structures, and the resulting low energy and temperature requirements of few tens of mK may thus be lifted to some extent by going to smaller structures.

The Hamiltonian used to describe this system is of the

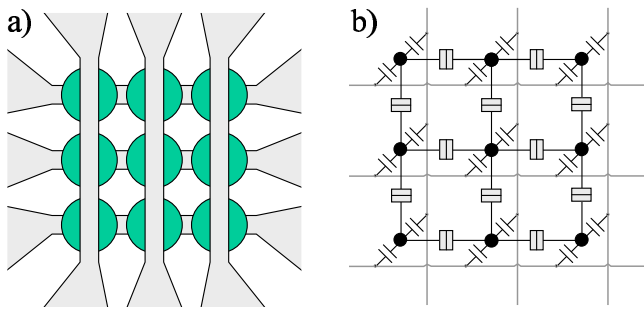


FIG. 1: Model system - 3×3 array: (a) schematic layout: circles represent quantum dots and the three horizontal and three vertical bars represent the gates which are connected to the outside world. (b), same as panel (a) but drawn as a capacitor and tunnel junction network, where black circles represent the qudots. The box symbols in between dots represent capacitive tunnel junctions.

extended Hubbard type

$$H = \sum_{i,\sigma} \varepsilon_{\sigma} c_{i\sigma}^{\dagger} c_{i\sigma} - \sum_{i,j,\sigma} t_{ij}^{\sigma} (c_{i\sigma}^{\dagger} c_{j\sigma} + c_{j\sigma}^{\dagger} c_{i\sigma}) + \frac{1}{2} \sum_{i,j} V_{ij} \hat{n}_i \hat{n}_j + \sum_i V_i \hat{n}_i, \quad (2)$$

where $\hat{n}_i \equiv c_{i\uparrow}^{\dagger} c_{i\uparrow} + c_{i\downarrow}^{\dagger} c_{i\downarrow}$ in the standard notation. The $\varepsilon_{(i)\sigma}$ refers to the local energy of the state σ on the $i = \{1, \dots, n\}$ identical dots and can be used to account for the Zeeman splitting of spins in an external magnetic field. For most cases, ε_{σ} is simply set to zero. The tunneling coefficients t_{ij}^{σ} are considered independent of the spin orientation, thus $t_{ij}^{\uparrow} = t_{ij}^{\downarrow} \equiv t_{ij}$, and unequal to zero only between nearest neighbors in the qudot network. The electrostatic energy in the last two terms of Eq. (2), i.e. the coefficients V_{ij} and V_i , are derived from the (total) capacitance matrix of the system (see App. A for more details).

Throughout this paper, the electronic system of qudots is considered to have, for simplicity, a fixed number of two electrons ($2e$) operating in it. Furthermore, since spin flip processes occur on a comparatively long time scale [2, 3, 4], they are neglected and thus the overall spin is considered constant. The correct statistics for exchange of the two electrons is taken into account by the fermionic creation (annihilation) operators $c_{i\sigma}^{\dagger}$ ($c_{i\sigma}$). Since spin is conserved, the basis for the two spin 1/2 particles ($2e$) is conveniently changed to singlet and triplet states which are also spin eigenstates. Fermionic statistics constrains the spatial wavefunction of the (triplet) singlet states under particle exchange to be (anti)symmetric, respectively. Henceforth, the spin index can be dropped completely, and the distinction between singlet and triplet states can be incorporated by using (fermionic) bosonic operators for (triplet) singlet states, respectively, with the constraint of two particle occupation in the system.

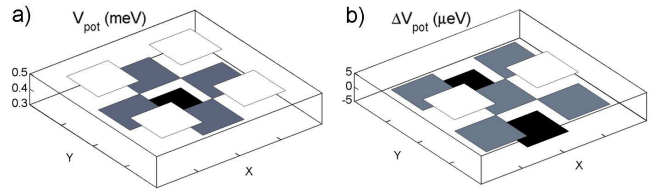


FIG. 2: Potential landscape for array in Fig. 1. (a) Single particle potential on array with no gate voltages applied ($V_g = 0$). (b) Change of single particle potential due to one specific set of applied gate voltages.

III. SINGLE QUBIT QUANTUM GATES

The 3×3 model introduced in the previous section is representative for a network with C_{4v} symmetry. With this geometrical symmetry, several states will have a natural 2-fold degeneracy. Having set up the total capacitance matrix for the system, the single particle potential landscape for the array is shown in Fig. 2a for the case of no gate voltages applied. The absence of nearest neighbors on the outer boundary results in an electrostatic potential well such that a single charge stays preferentially in the center of the array. Applying a peculiar pattern of gate voltages, the 90° symmetry of the potential can be broken which effectively alters the potential on the middle outer islands only; Fig. 2b depicts an example of such a situation.

A. Numerical Simulations

Adding a second charge to the 3×3 array leads to a competing effect of the potential well structure in Fig. 2a with Coulomb repulsion and the two charges push each other halfway outside (see Fig. 3d+e) resulting in two low-lying classically degenerate states with charges arranged either vertically (3d) or horizontally (3e). The eigenspectrum for the 3×3 system with two electrons and its dependence on the gate voltage pattern shown in Fig. 2b is plotted in Fig. 3a. The three different spin configurations for triplet states have exactly the same eigenspectrum. So looking at one specific triplet spin configuration, there is still an exact degeneracy in the ground state due to the spatial symmetry when no gate voltages are applied. The corresponding spatial configurations are shown in Fig. 3d+e. For the singlet states, however, a gap opens up. This gap originates from the distinct exchange symmetry in the spatial part of the wave function when compared to the triplet states. Taking as basis states those shown for the triplet manifold in Fig. 3d+e, it is clear that for the singlet subspace they mix into their symmetric and antisymmetric combinations (bonding/antibonding states) near the degeneracy point where no gate voltages are applied ($V_g = 0$). One can consider the tunneling part of the Hamiltonian as a

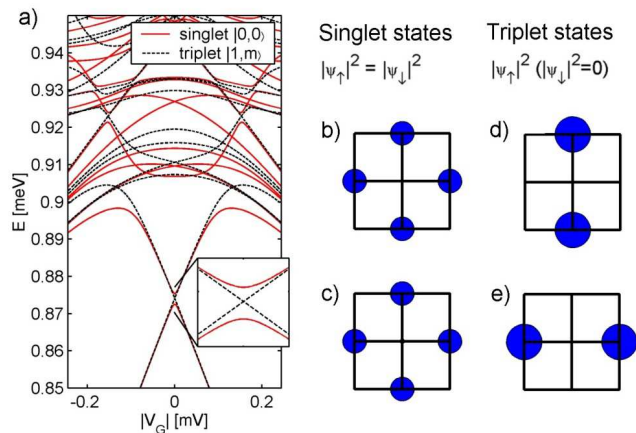


FIG. 3: (a) Energy level spectrum of the 3×3 system and dependence of the symmetry breaking pattern of gate voltages in Fig. 2b. Singlet states $|s, s_z\rangle = |0, 0\rangle$ are shown in red, while triplet states $|s, s_z\rangle = |1, m = \{+1, 0, -1\}\rangle$ are shown in dashed black. (b) and (c) Probability distribution over the 3×3 array of the ground pair (qu2LS) for singlet states. Notice equal probability for spin up and spin down ($|\psi_\uparrow|^2 = |\psi_\downarrow|^2$). (d) and (e) Lowest triplet states. Case chosen ($s_z = +1$) has only a spin up component (note, however, that spatial probability distribution is the same for the sixfold degenerate triplet states).

perturbation ($H = H_0 + V(t)$), so that the extra minus sign for particle exchange in the spatial part of the triplet wave functions has an interesting effect: the perturbative terms that mix the two basis states effectively cancel out, so that the degeneracy stays intact. The underlying reason, as seen below, is that due to the C_{4v} symmetry for each path there also exists a mirrored path where the particles are exchanged. However, for the singlet states, the perturbative terms all come with the same sign and add up. Thus the basis states effectively mix, resulting in the singlet states shown in Fig. 3b+c. The gap that opens then for the singlet states as a function of gate voltages, is properly described as an anticrossing in the level spectrum and this immediately opens the path towards generating Rabi oscillations in the system characterized by different charge configurations.

The gap between singlet states with no voltages applied ($\mathbf{V}_g = 0$) can be estimated using the Feshbach formalism [14] which is a well-suited approximation for a state space well separated from the remainder of the Hilbert space and can be thought of as a perturbative approach that builds on path histories in the Hilbert space. The lowest order term for weak tunneling t and consistent with the numerical data is given as

$$\delta \sim 32 \frac{t^4}{\Delta_0^3}, \quad (3)$$

where Δ_0 is the energy gap to the excited manifold ($\Delta_0 \simeq 0.03\text{meV}$ in Fig. 3a). This result can be visualized as four hops (t^4) needed at the cost of at least Δ_0 for each of the

three intermediate states (Δ_0^{-3}); further, the prefactor gives the number of possible low energy paths to go from one basis state to the other including particle exchange symmetry.

A numerical simulation of the state evolution that makes use of the anticrossing of the singlet state is shown in Fig. 4. The state of the qu2LS is represented by a three dimensional vector in the Bloch sphere [1] where the (initial) eigenstates for $\mathbf{V}_g = 0$ are taken as the basis for this representation. Note that this is a slightly modified definition of the Bloch vector, insofar as there is a reservoir of higher lying states accessible to the system. Panels (a+b) show the *path* of the Bloch vector as three sequential qubit operations were performed: the first and the last operation are based on the symmetry breaking gate voltage pattern shown in Fig. 2b, which rotate the Bloch vector around the z axis, the horizontal circular path in panel (a). For demonstrational purposes, the second operation is based on tunable tunneling (an effective σ_x gate in the pseudo-spin space of the qubit, see below). This second operation rotates the Bloch vector around the x -axis and together with the first operation allows one to rotate the Bloch vector anywhere in the Bloch sphere as required for single qubit operations. Panel (c) shows the evolution of the real space probability distribution during the second operation. The two basis states in Fig. 3d+e are nicely rotated into each other over a time consistent with the nature of the Rabi oscillations. Typical rise-times for the voltage gate that do not mix in higher lying states are well below the 1 ps range, while if one were to tune the tunneling, the minimal rise-times for adiabatic switching would require times in the 100ps range, in order to limit the admixing of higher lying states. The adiabatic regime considered here is clearly seen in the Bloch sphere representation of Fig. 4b by observing that the length of the Bloch vector is reduced to less than one in the intermediate gate operation. On return to the initial parameters, this amplitude temporarily lost to the bath is regained, however.

B. Rabi Oscillations and 2nd Quantum Gate

Qubits are conveniently mapped onto the spin 1/2 formalism using Pauli matrices [1, 12]; the system is described by a pseudospin which can be rotated in $3D$ space by applying perturbations which effectively act as magnetic field along different directions (note that there is no real magnetic field and that the real spin of the two electron system is taken care of by the singlet and triplet states). An arbitrary single qubit operation thus requires the realization of two distinct rotations in the $3D$ pseudo-spinor space. This translates to two linearly independent combinations of the three Pauli matrices $\sigma_{\{x,y,z\}}$ required to implement the necessary quantum gates. σ_z is easily implemented using the gate voltages and thus applying different potentials to different regions in the qudot array as outlined in the previous section. Further, if one

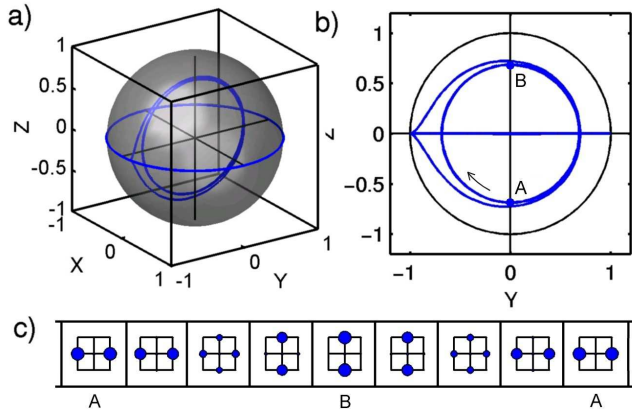


FIG. 4: Coherent manipulation of the singlet state under gate action - (a) Evolution of the qubit in the Bloch sphere representation after projection onto the basis of the (initial) eigenspectrum at $\mathbf{V}_g = 0$. The Bloch sphere is shown in black, and the evolution of the Bloch vector in the qu2LS is shown in blue. (b) Same as panel (a), but side view, showing the slight size reduction due to the adiabatic interaction with the higher lying reservoir of states. (c) Coherent Rabi oscillations for the sequence $A \rightarrow B \rightarrow A$ in panel (b) in the direction indicated with $t = 10\mu\text{eV}$. The probability distribution in real space is shown for the 3×3 array over equally spaced time intervals in a total time window of 0.56ns which corresponds to one period for this tunneling based action.

considers the tunneling t to be approximately constant, like in lithographically grown qudot structures with the tunneling determined by oxide layers, one may ask if it is possible to obtain the second qugate by applying a peculiar pattern of only capacitively coupled voltage gates. The answer turns out negative in the sense that either the second gate (σ_x) is orders of magnitude weaker than the first gate (σ_z), or it compromises the two-level ground state system such that at least one initially well split off eigenstate comes within gap distance to the qubit encoding subspace [13].

As a way to illustrate this result in the 3×3 system of Fig. 1a, all six gate voltages were sampled randomly within their parameter space and over a significant range of tunneling coefficient t values. The results are shown in Fig. 5. From panel (a), the region of the intact two-level system involving the ground state is identified as the region where $\delta(V) \ll \Delta(V)$ and thus $t \leq 5\mu\text{eV}$; $\delta \equiv E_1 - E_0$ and $\Delta \equiv E_2 - E_1$ are the energy differences of the lowest three states. It is then clear that the condition $\delta(V) \gtrsim \Delta(V)$ makes the assumption of an isolated qu2LS no longer valid. Panel (b) to the right of Fig. 5 shows the effective pseudo-magnetic fields defined via the most general effective Hamiltonian in the qu2LS, namely $H \equiv a1 + \vec{\mathcal{B}} \cdot \vec{\sigma}$, where $\vec{\mathcal{B}} \equiv \vec{\mathcal{B}}_{\text{eff}}$ stands for the effective equivalent of a magnetic field. \mathcal{B}_z can clearly be turned on and off by the gate voltages and ranges from zero to the value limited by the applied voltages. Yet, \mathcal{B}_x is overwhelmingly set by the tunneling t and hardly

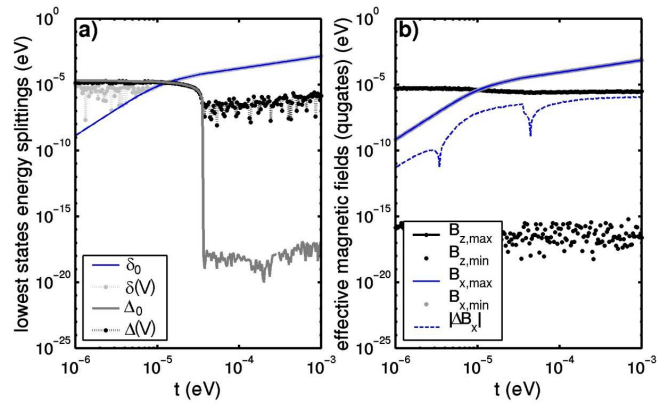


FIG. 5: Numerical exploration of effective (pseudo-) magnetic fields from a random sequence of gate voltages (4096 configurations for every t value). (a) Energy level splitting between the lowest two eigenstates (the qu2LS), δ , as well as the level splitting between the 2nd and the 3rd eigenstate, Δ , shown with and without gate voltages applied. A well behaved two level system exists for $t \lesssim 0.5 \times 10^{-5}\text{eV}$, while for larger t higher lying states cross over. (b) Sampling the gate voltages randomly, the minimum and maximum pseudo-magnetic fields achieved are recorded ($H = a1 + \vec{\mathcal{B}}\vec{\sigma}$, and thus $\vec{\mathcal{B}}$ has units of energy). Since $\mathcal{B}_{x,\text{min}}$ and $\mathcal{B}_{x,\text{max}}$ are very similar, the difference $\Delta\mathcal{B}_x$ is shown explicitly by the blue dashed line. $\mathcal{B}_{z,\text{min/max}}$ values are clearly discernible. Note that the \mathcal{B}_x is directly related to the gap in the ground state (δ_0 in panel (a))

responds to different applied voltages. In other words, although we have access to a variety of gate voltages and diverse ranges, the fixed t -value is the one that essentially determines the σ_x gate. As t cannot be varied, it negates the qubit control one needs over the entire Bloch sphere. The range of \mathcal{B}_x values obtained by varying local voltages is so narrow that it is hardly visible in Fig. 5b. In order to see the difference between the maximum and minimum value of \mathcal{B}_x achieved, their difference $|\Delta\mathcal{B}_x|$ is plotted separately: the first dip in this curve is related to a change in sign in $\Delta\mathcal{B}_x$, while the second kink is already well beyond the two-level regime and originates in other higher lying states taking over the ground state.

The numerical results show that despite having access to a large set of voltage gates, the second qugate *cannot* be implemented electrostatically under the assumptions of constant tunneling and no real external magnetic field [13]. One may argue, that this happens because of the peculiar geometry chosen and that there may be other geometries which would respond differently. That this is not the case will be shown in the following section.

IV. ELECTROSTATIC INTERACTIONS WITH GATES

From an analytical point of view, some general statements can be made on the charge states considered here.

From our description of the situation above, we can formulate the following two points:

- B1. Encoding the qubit in the charge and thus in the spatial wave function, demands that the basis of the ground state pair be formed from two spatially separated wave functions.
- B2. Implementation of a second qugate via electrostatic means with the tunneling t kept constant and with no real external magnetic field [13] results in compromising of the two-level low-energy system, invalidating its use.

We can in fact demonstrate that these two points are true *in general*, as evidenced by the specific geometry above. In order to show this, we will use the following statements:

- C1. The ground state of any state (single particle, singlet or triplet) for a real (not complex) Hamiltonian must be nodeless, where for the states with more than one particle one must consider the restricted space $\Omega \equiv \vec{r}_1 < \vec{r}_2 < \dots$ only within some unique sorting scheme, where \vec{r}_i points to the location of particle i (this restriction is necessary since for example on the overall space, the triplet states have an intrinsic node due to the particle exchange symmetry).
- C2. If a matrix element $\langle \psi_1 | V | \psi_2 \rangle$ is $\neq 0$ for a local potential, then for $\psi_1 \neq \psi_2$ at least one of the two wave functions must have a node within the space Ω , and thus must be split off from the ground state itself.

The argument for statement (C1) is similar to one found in [15]. The statement follows from the observation that any eigenstate $\psi(\vec{r}_1, \vec{r}_2)$ with a node within Ω has a counterpart $|\psi|$ which has the same energy expectation value $\int_{\Omega} |\psi| \cdot H \cdot |\psi| = E = \int_{\Omega} \psi H \psi$ and thus by the variational principle, the ground state must be always nodeless or, at least, can be chosen as such. Statement (C2) is shown as follows: since $\int_{\Omega} \psi_1^*(\vec{r}_1, \vec{r}_2) V(\vec{r}_1, \vec{r}_2) \psi_2(\vec{r}_1, \vec{r}_2) \neq 0$ with the local potential $V(\vec{r}_1', \vec{r}_2'; \vec{r}_1, \vec{r}_2) \equiv V(\vec{r}_1, \vec{r}_2) \delta(\vec{r}_1' - \vec{r}_1) \delta(\vec{r}_2' - \vec{r}_2)$ there must some region in space where both ψ_1 and ψ_2 are $\neq 0$ simultaneously. Yet, since ψ_1 and ψ_2 are orthogonal eigenfunctions, in order for $\langle \psi_1 | \psi_2 \rangle$ to be $= 0$ there must be still another region in space with both ψ_1 and ψ_2 unequal to zero but with a different sign compared to the first region. Thus either ψ_1 or ψ_2 must switch sign from one region to the other.

With this, statement (B1) follows from the observation that for some specific set of parameters (within the working-range of the qubit) the ground state is degenerate; thus utilizing statement (C1), both of these ground states must be nodeless. Yet, they must be also orthogonal to each other, and so similar to statement (C2),

ψ_1 and ψ_2 can be chosen such that $\psi_1 = 0$ where $\psi_2 \neq 0$ and vice versa. This is what is meant by spatially separated wave functions. Furthermore, since this ground state pair is supposed to be sufficiently decoupled from the remaining states, this situation may only change slightly during gate operations.

For statement (B2), the Feshbach formalism is employed once more. In the matrix representation, the Hamiltonian of the qubit system with an isolated subspace with index $\{1, 2\}$ is given by

$$H = \begin{pmatrix} \begin{array}{cc|ccc} \varepsilon_1(\mathbf{V}_g) & 0 & \dots & H_{1k'}(t) & \dots \\ 0 & \varepsilon_2(\mathbf{V}_g) & \dots & \dots & \dots \\ \vdots & \vdots & \ddots & \vdots & H_{kk'}(t) \\ H_{1k'}^*(t) & \vdots & \dots & \varepsilon_k(\mathbf{V}_g) & \dots \\ \vdots & \vdots & H_{kk'}^*(t) & \vdots & \ddots \end{array} \\ \equiv \begin{pmatrix} H_{PP}(\mathbf{V}_g) & H_{PQ}(t) \\ H_{PQ}^\dagger(t) & H_{QQ}(t, \mathbf{V}_g) \end{pmatrix} \end{pmatrix} \quad (4)$$

with H_{PP} the projection of the Hamiltonian onto the 2D ground state space where $\varepsilon_1 = \varepsilon_2$ for $\mathbf{V}_g = 0$ with \mathbf{V}_g the set of external gate potentials. In this spatial representation, the potential \mathbf{V}_g enters only in the diagonal of the Hamiltonian and, furthermore, the Hamiltonian is diagonal when $t = 0$. So there is no coupling of H_{PP} to the remaining space for $t = 0$ since $H_{PQ}(0) = 0$. From this structure of the Hamiltonian, the first qugate (σ_z) is easily realized by choosing \mathbf{V}_g such that $\varepsilon_1 \neq \varepsilon_2$; the second qugate, however, must be realized through coupling to the remaining space. For simplicity but without restricting the case, a \mathbf{V}_g is chosen that leaves ε_1 and ε_2 constant or just shifts them together uniformly; the effective two-level Hamiltonian created by the Feshbach formalism effectively folds the remaining Hilbert space into the reduced Hamiltonian H_{PP} and thus creates a shift in the diagonal, as well as generating the off-diagonal elements. The latter terms can be straightforwardly related to the σ_x which gives the splitting in Eq. (3). Thus by comparison, the effective second qugate for singlet states is approximated by

$$\mathcal{B}_x \approx 32 \frac{t^4}{[\Delta(\mathbf{V}_g)]^3}$$

where $\Delta(\mathbf{V}_g) \equiv \Delta_0 + \Delta\varepsilon(\vec{V}_g)$ is the gap with applied \mathbf{V}_g , and $|\Delta\varepsilon/\Delta_0| \ll 1$, so that the second gate is approximated by

$$\mathcal{B}_x \approx 32 \frac{t^4}{\Delta_0^3} \cdot \left(1 - \frac{3\Delta\varepsilon(\mathbf{V}_g)}{\Delta_0} \right) \quad (5)$$

Note that this is a maximum estimate since all relevant higher lying energies are supposed to behave collectively. Yet, as seen from Eq. (5), this second qugate has a much weaker dependence on the gate voltages since it must be mediated by the coupling t , while the first qugate is

sensitive to the gate voltages as $\Delta\varepsilon(\mathbf{V}_g)$ directly. For the ground state two-level system to be sufficiently ideal in the sense of decoupled from the rest of the system, it must hold that $t/\Delta_0 \ll 1$ and also $|\Delta\varepsilon/\Delta_0| \ll 1$ for the gate operation to not interfere with the higher lying states. The consequence is that the initial splitting for the singlet states is small and the effect of the second qugate only changes this splitting by a fraction which is an order of magnitude smaller. In order to get a significant contribution, the second condition $|\Delta\varepsilon/\Delta_0| \ll 1$ would have to be lifted but that obviously sacrifices the two-level system altogether. This proves statement (B2).

Local electrostatic interaction of voltage gates with a qubit system is therefore not sufficient for a full set of single qubit rotations. However, revision of the arguments brought forward clearly leaves two ways out of this dilemma: first, the gap (\mathcal{B}_x) is controlled by the tunneling. Thus tunable tunneling allows for the second qugate needed as is well-known [10]. Second, the Hamiltonian was assumed to be real. The argument of a nodeless ground state wave function very much relies on that fact since for a real wave function a sign change is only possible via a transition through zero while in the complex case this is no longer required. With this, statement (B1) becomes irrelevant, and the freedom on $\langle\psi_1|V|\psi_2\rangle \neq 0$ is greatly increased. Specifically, an external magnetic field which makes the Hamiltonian complex, will in fact not increase the initially existent (but constant!) σ_x qugate for singlet states, but it can reduce it to zero. Eventually, this is again equivalent to an effectively tunable tunneling [13].

V. CONCLUSIONS

The use of spatial wave functions to encode quantum bits has been analyzed with respect to capacitive electrostatic interactions. With emphasis on systems such as lithographically grown arrays where the tunneling is fixed to a great extent by the thickness of the tunnel barriers (oxide layers) used, it was shown that with constant tunneling t and no external magnetic field present, the single qubit operations from a system built this way are severely limited. The analysis shows that a full set of single qubit operations requires either a tunable tunneling or an external magnetic field which makes the wave function complex and thus introduces further flexibility. A uniform external magnet field applied to one qubit, on the other hand, needs to be sufficiently localized with respect to an ensemble of qubits eventually needed. This is a very challenging experimental task. The parameters

for the dot-dot capacitances chosen give energy scales for the tunneling operations in the constrained two-level system in the few μeV range. Capacitances of about 45aF are related to dimensions of a few hundred nm. Therefore, still possible smaller sizes leave room for increased energy scales.

Acknowledgments

We acknowledge helpful discussions with J. Heremans and D. Phillips, as well as support from NSF Grant NIRT 0103034, and the Condensed Matter and Surface Sciences Program at Ohio University.

APPENDIX A: CAPACITANCE MATRIX AND QUDOT INTERACTION

The total capacitance matrix of the system consisting of dots and gates is written as

$$C_{tot} \equiv \begin{pmatrix} C_{dot-dot} & C_{dot-gate} \\ C_{gate-dot} & C_{gate-gate} \end{pmatrix} \equiv \begin{pmatrix} C_{11} & C_{12} \\ C_{21} & C_{22} \end{pmatrix} \quad (\text{A1})$$

where the matrix has been decomposed into convenient block notation which separates the dot-dot and dot-gate interactions. For a network of capacitors connecting pairs of objects (dots or gates), the individual matrix elements are given as

$$C_{ij}^{tot} = \begin{cases} C_{i,0} + \sum_{j' \neq i}^{dots, gates} C(i \leftrightarrow j') & \text{for } i = j, \\ -C(i \leftrightarrow j) & i \neq j. \end{cases} \quad (\text{A2})$$

where $C_{i,0}$ is the necessary self-capacitance of the i -th object and $C(i \leftrightarrow j)$ is the capacitor value between the two objects i and j . Here, the capacitance matrix is approximated by a network of nearest neighbor capacitors where the specific capacitance values enter as parameters to the model. With the block matrix notation given in Eq. (A1), the coefficients V_{ij} and V_i for the Hubbard Hamiltonian in Eq. (2) follow as

$$V_{ij} = e^2 [C_{11}^{-1}]_{ij}, \quad V_i = e [\mathbf{V}_g \cdot C_{21} C_{11}^{-1}]_i \quad (\text{A3})$$

The interaction of the dots to the gates is mediated as expected by the off-diagonal block C_{21} of the total capacitance matrix and is linear in the applied set of gate voltages $\mathbf{V}_g = \{V_{g,1}, V_{g,2}, \dots\}$.

-
- [1] M. Nielsen, I. Chuang, *Quantum Computation and Quantum Information*, Cambridge University Press (2000).
 [2] J. Levy, Phys. Rev. A **64**, 052306 (2001).

- [3] J. Gordon and K. Bowers, Phys. Rev. Lett. **1**, 368 (1958).
 [4] J. Kikkawa, I. Smorchkova, N. Samarth, D. Awschalom, Science **277**, 1284 (1997).
 [5] T. Hayashi, T. Fujisawa, H. D. Cheong, Y. H. Jeong,

- Y. Hirayama, Phys. Rev. Lett. **91**, 226804 (2003).
- [6] H. Goan, G. Milburn, Phys. Rev. B **64**, 235307 (2001).
- [7] L. DiCarlo, H. J. Lynch, A. C. Johnson, L. I. Childress, K. Crockett, C. M. Marcus, cond-mat/0311308 (2003).
- [8] M. Devoret and R. Schoelkopf, Nature **406**, 1039 (2000).
- [9] G. Toth and C. S. Lent, Phys. Rev. A **63**, 052315 (2001).
- [10] S. Gardelis, C. G. Smith, J. Cooper, D. A. Ritchie, E. H. Linfield, Y. Jin, Phys. Rev. B **67**, 033302 (2003).
- [11] M. Storcz, F. Wilhelm, Phys. Rev. A **67**, 042319 (2003).
- [12] L. Ballentine, *Quantum Mechanics* (World Scientific, Singapore, 1999).
- [13] It turns out it is also possible to control the effective tunneling in the qudot array via the application of an actual magnetic field. We will discuss that possibility elsewhere.
- [14] H. Feshbach, *Annals of Physics (N.Y.)*, **19**, 287 (1962).
- [15] J. Slater, H. Statz, G. Koster, Phys. Rev. **91**, 1323 (1953).